IFT 252/77



# DENSITIES, FORM FACTORS, TRANSITIONS AND MULTIPOLE MOMENTS IN THE s-d SHELL , WITH THE SKYRME FORCE*

D.R.de Oliveira and S.S.Mizrahi+
Instituto de Física Teórica, São Paulo,SP,
Brasil++

Instituto de Física Teórica, Rua Pamplona, 145
Caixa Postal-5956
01405-São Paulo-Brasil
September - 1977

* Work partially supported by FINEP, Brasil.

+ Fellowship from FAPESP, São Paulo, Brasil.

++ Postal Address: Caixa Postal 5956, 01405 - São Paulo.

# DENSITIES, FORM FACTORS, TRANSITIONS AND MULTIPOLE MOMENTS IN THE s-d SHELL, WITH THE SKYRME FORCE*

D.R. de Oliveira and S.S. Mizrahi+
Instituto de Física Teórica, São Paulo,SP.,Brasil++

Abstract : This paper reports the nuclear densities, radii, multipole moments, form-factors and transition probabilities obtained for the A = 4n type of nuclei in the s-d shell, using the Hartree-Fock wave functions calculated in Ref.(1) with the Skyrme force. Experimental data and theoretical values derived by others are shown for comparison.

---

* Work partially supported by FINEP, Brasil.

+ Fellowship from FAPESP, São Paulo, Brasil.

++ Postal Address : Caixa Postal 5956, 01405 - São Paulo.

## 1. Introduction

In our previous paper[1] we applied the Hartree-Fock (HF) approximation with the Skyrme force to the A = 4n type of nuclei in the s-d shell. We used the Peierls and Yoccoz projection method to obtain wave functions of good angular momentum, energy levels and transition probabilities within the ground state band. The results were better than those obtained with more sophisticated two-body interactions. We had to assume the $O^{16}$ to be an inert core and the basis of independent particle wave functions was truncated to the s-d subspace. Time reversal and charge symmetry were also assumed.

The two-body part of the Skyrme[2] interaction is written in configuration space as

$$\begin{aligned} v_{12}(\vec{r}_1-\vec{r}_2) = {} & t_0(1+x_0 P^\sigma)\,\delta(\vec{r}_1-\vec{r}_2) + \tfrac{1}{2} t_1 (1+x_1 P^\sigma)\cdot \\ & \left[\vec{k}^{\dagger 2}\,\delta(\vec{r}_1-\vec{r}_2) + \delta(\vec{r}_1-\vec{r}_2)\,\vec{k}^2\right] + \\ & + t_2\,\vec{k}^\dagger\cdot\delta(\vec{r}_1-\vec{r}_2)\,\vec{k} + \\ & + i W_0 (\vec{\sigma}_1+\vec{\sigma}_2)\,\vec{k}^\dagger \times \delta(\vec{r}_1-\vec{r}_2)\,\vec{k}\ , \end{aligned} \tag{1}$$

where $\vec{k}^\dagger$ and $\vec{k}$ are relative momentum operators; $P^\sigma$ is the spin-exchange operator, $\vec{\sigma}_1$ and $\vec{\sigma}_2$ are Pauli spin matrices. The three body term of the Skyrme force is also of zero-range

$$v_{123}(\vec{r}_1-\vec{r}_2, \vec{r}_2-\vec{r}_3) = t_3\,\delta(\vec{r}_1-\vec{r}_2)\,\delta(\vec{r}_2-\vec{r}_3) \tag{2}$$

and, for HF calculations of even-even nuclei, this force is equivalent to a two-body density dependent interaction

$$w_{12}(\vec{r}_1-\vec{r}_2)\,\rho\left(\frac{\vec{r}_1+\vec{r}_2}{2}\right) = \frac{1}{6}\,t_3\,(1+P^\sigma)\,\delta(\vec{r}_1-\vec{r}_2)\,\rho\left(\frac{\vec{r}_1+\vec{r}_2}{2}\right) \qquad (3)$$

In Ref.(1) we discuss how we performed the fitting to nuclear properties, that lead us to the following values for the parameters:

$t_0 = -1115.5$ MeVfm$^3$ $\qquad$ $t_1 = 314.6$ MeVfm$^5$

$t_2 = -106.7$ MeVfm$^5$ $\qquad$ $t_3 = 14992.8$ MeVfm$^6$

$\chi_0 = \chi_1 = 0.8$ $\qquad$ $W_0 = 68.1$ MeVfm$^5$

What we found was compared to the available experimental data and to some theoretical results derived by others.

D. Vautherin[3] used two sets of parameters determined by Brink and himself (VB-I and VB-II) for the Skyrme force. A modified version of Negele's effective interaction was used by Zofka and Ripka[4] (ZR). Moszkowski[5] also studied some s-d shell nuclei with his Modified Delta Interaction (MDI). We quote some of their results.

## 2. Multipole Expansion of the Nuclear Density

The density of states distribution of a nucleus with A nucleons is given by

$$\rho(\vec{r}) = \sum_{i=1}^{A} |\phi_i(\vec{r})|^2 \,, \qquad (4)$$

the summation being over the occupied states described by the Hartree-Fock single particle wave functions $\phi_i(\vec{r})$. The above expression can be developed to the final form

$$\rho(\vec{r}) = \sum_L \rho_L(r)\, P_L(\cos\theta) \quad , \tag{5}$$

where the multipolar expansion coefficient is

$$\rho_L(r) = \rho_{O^{16}}(r)\, \delta_{L0} + \rho_L^{VN}(r) \quad . \tag{6}$$

The first contribution comes from the inert core and the second is from the valence nucleons, namely

$$\rho_{O^{16}}(r) = \frac{1}{\pi} \sum_{(n\ell)=(00)(01)} (2\ell+1)\, R_{n\ell}^2(r) \tag{7}$$

and

$$\rho_L^{VN}(r) = \left(1+(-1)^L\right) \frac{2L+1}{2\pi} \sum_{\substack{n\ell j m \\ n'\ell' j'}} \rho^{HF}_{\alpha'\alpha}\, R_{n\ell}(r)\, R_{n'\ell'}(r)$$
$$\left[(2\ell+1)(2\ell'+1)\right]^{1/2} (L\,0\,\ell'\,0 \mid \ell\,0)\,(L\,0\,j'\,m \mid j\,m) \tag{8}$$
$$W(L\,\ell'\,j\,\tfrac{1}{2};\,\ell\,j')$$

Besides the Clebsch-Gordan and Racah coefficients, the $R_{n\ell}(r)$ are radial wave functions, $\rho^{HF}_{\alpha\alpha'}$ is the HF density of states; $\alpha$ stands for the set of harmonic oscillator quantum numbers $n, \ell, j, m$. In the s-d shell, the contributing L values are L = 0 (monopole),

L = 2 quadrupole) and L = 4 (hexadecapole).

As we neglect the Coulomb interaction and N = Z, the density of protons will be $\rho^p(\vec{r}) = \frac{1}{2}\rho(\vec{r})$, where the total density $\rho(\vec{r})$ is given by (5). Corrections due to the center of mass motion and to the finite size of proton[6] were taken into account, such that one obtains the nuclear charge density distribution $\rho^c(\vec{r})$, which can be also written as a multipole expansion. The new coefficient $\rho_L^c(r)$ is a function of the old one given by expressions (6), (7) and (8).

The charge density distribution coefficients for L = 0,2,4 are shown in Figure 1 for $Ne^{20}$, $Mg^{24}$, $Si^{28}$ and $S^{32}$. Comparison with the experimental data will be made through the electron scattering form factors as the experimental densities are derived from them.

FIGURE 1

3. Radii

The nuclear mass and charge distributions expressions are

$$\langle r_M^2 \rangle = \frac{4\pi}{A} \int_0^\infty \rho_o(r)\, r^4\, dr \qquad (9)$$

and

$$\langle r_c^2 \rangle = \frac{4\pi}{A} \int_0^\infty \rho_o^c(r)\, r^4\, dr \ , \qquad (10)$$

respectively. $\rho_0(r)$ is given by (6) for L = 0, and $\rho_0^c(r)$ is the L = 0 expression for the charge distribution, taking into account the corrections due to the center of mass motion and to the finite size of proton.

In Table I we compare the experimental values of the nuclear charge r.m.s. radius for $Ne^{20}$, $Mg^{24}$, $Si^{28}$, $S^{32}$ and $Ar^{36}$ with the ones obtained by various authors.

The mass radius, not including the corrections, is also shown; one sees that the finite size of proton and the center of mass motion corrections increase the radius value .

The expressions depend on the harmonic oscillator constant b. We used the Blomqvist-Molinari[7] formula to calculate the value of b for each nucleus. What we found is in very good agreement with the data, indicating that their formula works quite well for light nuclei.

TABLE I

4. Intrinsec Multipole Moments

The nuclear charge intrinsec quadrupole and hexadecapole moments are defined by the expectation values

$$Q_0^c = 2 \langle \Phi_0 | \hat{Q}_0^2 | \Phi_0 \rangle \qquad (11)$$

and

$$H_o^c = \langle \Phi_o | \hat{Q}_o^4 | \Phi_o \rangle \quad , \tag{12}$$

where $|\Phi_o\rangle$ is the Hartree-Fock ground state, the operators having the well-known forms

$$\hat{Q}_o^2 = \frac{1}{e} \sum_{i=1}^{Z} \sqrt{\frac{4\pi}{5}}\, e_i\, r_i^2\, Y_{20}(\Omega_i) \tag{13}$$

and

$$\hat{Q}_o^4 = \frac{1}{e} \sum_{i=1}^{Z} \sqrt{\frac{4\pi}{9}}\, e_i\, r_i^4\, Y_{40}(\Omega_i) \tag{14}$$

Assuming that the proton and neutron wave functions are equal, plus the fact that N = Z, we can write

$$Q_o^c = (1 + \alpha_p + \alpha_n)\, \frac{8\pi}{5} \int_0^\infty \rho_2^c(r)\, r^4\, dr \tag{15}$$

$$H_o^c = (1 + \alpha_p + \alpha_n)\, \frac{4\pi}{9} \int_0^\infty \rho_4^c(r)\, r^6\, dr \; . \tag{16}$$

The nuclear charge distribution densities are the ones including the corrections mentioned before. The proton and neutron effective charge corrections, $\alpha_p$ and $\alpha_n$, were taken as 0.5. One sees that $Q_o^c$ ($H_o^c$) measures the quadrupole (hexadecapole) deformation of the nu-

clear harge distribution. Depending of the sign of $Q_o^c$ being positive o: negative, the deformation will be prolate or oblate, respectively.

The quadrupole moments are in Table II; the best comparison with the experimental data was reached by Vautherin, with the VB-II set of parameters, also by Zofka and Ripka and this work. Our values of the hexadecapole moments in Table III are too low by a factor of two compared to the experimental ones.

TABLE II and TABLE III

5. Electron-nucleus scattering form factors

In the Born approximation, the elastic and inelastic form factors are given by the following expressions:

$$F_{el}^2(k) = \frac{4\pi}{Z^2}\left|\int_0^\infty j_0(kr)\,\rho_o^c(r)\,r^2\,dr\right|^2 \qquad (17)$$

and

$$F_{0\to J}^2(k) = \frac{4\pi}{(2J+1)^2}\,\frac{(1+\alpha_p+\alpha_n)}{Z^2}\,\frac{C_J^2}{C_o^2}\cdot \left|\int_0^\infty j_J(kr)\,\rho_J^c(r)\,r^2\,dr\right|^2 \qquad (18)$$

The momentum transfer is $\hbar k$ ; the target nucleus has Z protons, the

ground state spin is zero and J is the angular momentum of its final excited state; these excited states are projected from the HF wave function, the $C_J$'s being their normalization constants.

FIGURE 2

We show the elastic form factors in Figure 2.

The experimental points for $Mg^{24}$, $Si^{28}$ amd $S^{32}$ are from Ref.(9); for $Ne^{20}$ they are from Ref.(11). The curves reproduce quite well the experimental points before the diffraction minimum. This region of low momentum transfer corresponds to the nuclear surface, which is, therefore, well described by our wave functions, justifying the good values obtained for the nuclear charge radii. After the first minimum, the curves have a peak localized below the experimental points, except for $Ne^{20}$. Ripka found similar results, which may not be due to the Born Approximation, as Ford, Braley and Bar-Touv[12] also obtained this behaviour employing a better approximation. This region corresponds to high nuclear densities and the discrepancies are attributed to the fact that the Hartree-Fock wave functions do not contain short range correlations. It has been verified[13] that, when Jastrow correlations are introduced in the nuclear wave functions, the form factor second peak value increases.

The form factors corresponding to the inelastic scattering, with a $0^+ \longrightarrow 2^+$ nuclear transition, are shown in Figure 3.

FIGURE 3

The experimental points were taken from the same references as in the elastic case. This form factor depends on the charge quadrupole density shown in Figure 1. Some authors[12] suggest that one should increase the number of the shell model basis states in order to improve the results. In our case, it seems that only the 1s-0d states were enough to account for $Si^{28}$. The other nuclei may have a bigger quadrupolar deformation, thus requiring more single particle states.

In Figure 4, we show the $0^+ \longrightarrow 4^+$ transition form factors only for $Ne^{20}$ and $Si^{28}$, which are not in good agreement with the experimental points. There are no data available for the other nuclei we studied.

FIGURE 4

6. Transition Probabilities: In the limit of zero momentum transfer, the form factor for the $0^+ \longrightarrow J^+$ level excitation is related to the corresponding reduced electric transition probability by

$$B(EJ, k \to 0, 0^+ \to J^+) = Z^2 \lim_{k \to 0} \frac{[(2J+1)!!]^2}{k^{2J}} F^2_{0^+ \to J^+}(k) \quad (19)$$

$$= \frac{1}{16\pi} \frac{C_J^2}{C_o^2} \left(Q_o^c\right)^2 . \qquad (20)$$

A more general expression can be written starting from the definition[14],

$$B(EJ, 0^+ \rightarrow J^+) = \frac{1}{2J+1} \sum_M \left| \langle 2M | \hat{Q}_M^2 | 00 \rangle \right|^2 , \qquad (21)$$

where the final and initial states have well defined angular momentum, projected from the HF ground state wave function; $\hat{Q}_M^2$ is the electric quadrupole one-body operator. The matrix element becomes an expression which is evaluated after inserting a complete set of states, namely, the HF ground-state, the 1p-1h states, the 2p-2h states, etc. The particle-hole excitations involving two or more particles do not contribute. With the 1p-1h terms, the results were shown in Ref.(1). Without the 1p-1h terms, i.e., keeping only the H-F ground state in the complete set, it can be shown that the expression (21) will reduce to (20). In Table IV we show the results from each formula and the experimental values. For $Si^{28}$ the best theoretical value occurs when the expression (20) is used. This is consistent with the excellent fitting obtained for the $0^+ \rightarrow 2^+$ scattering form factor shown in Fig.(3).

TABLE IV

## 7. Conclusions

The results presented here are quite satisfactory in spite of the approximations we had to make concerning the inert core, as discussed in Ref.(1), plus the fact that the calculation was restricted to the s-d shell states.

The nuclear radii were in good agreement with the experimental values. The harmonic oscillator parameter b was not adjusted to reproduce the best radius. The value of b was fixed for each nucleus, given by the formula of Blomqvist and Molinari, which works well for light nuclei.

The best values for the quadrupole moments were obtained in the case of $Si^{28}$ and $S^{32}$, the other nuclei presented a 10-20% deviaton from experiment. With the usual nucleon effective charge we could not reproduce the hexadecapole moments; this could be attributed to the small subspace we worked with.

The elastic form factor has been well reproduced up to the first minimum, suggesting that, in the HF approximation, the nuclear long range correlations are correctly described by the Skyrme interaction. Except for $Si^{28}$, we failed to reproduce the inelastic form factors for the $0^+ \rightarrow 2^+$ transition, what is consistent with the quadrupole moments results.

A more complete study of nuclear properties in the HF approximation, with the Skyrme force, should be performed in a larger basis of single

particle states, without the inert core hypothesis, but including short range correlations.

References


1. D.R. de Oliveira and S.S. Mizrahi, Rev. Bras. Fís, 3,(1977).
2. T.H.R. Skyrme, Phil.Mag. 1, 1043(1956).
3. D. Vautherin, Phys. Rev. C7, 296(1973).
4. J. Zofka and G. Ripka, Nucl. Phys. A168, 65(1971).
5. S.A. Moszkowski, Phys. Rev. C2, 402(1970).
6. R. Hofstadter and E.E. Chambers, Phys. Rev. 103, 1454(1956).
7. J. Blomqvist and A. Molinari, Nucl. Phys. A106, 545(1968).
8. J. Moreira et.al., Can. Journ. Phys. 49, 1434(1971).
9. G.C. Li et.al., Phys. Rev. C9, 1861 (197 ).
10. Y. Torizuka et.al., Phys. Lett. 36B, 9(1971).
11. G. Ripka, "Proc. Int. Nucl. Struc. Studies", Sendai, Ed. K. Khoda and H. Ui, 1972.
12. W.F. Ford, R.C. Braley and J. Bar-Touv, Phys. Rev. C4, 2099(1971).
13. D.A. Sparrow and W.J. Gerace, Nucl. Phys. A145, 289(1970).
14. S.A. Moszhowski, "Alpha-Beta-Gamma Ray Spectroscopy", Vol.2, North-Holland,(1968).
15. A. Nakada and Y. Torizuka, Journ. Phys. Soc. Japan 32, 1(1972).
16. H.C. Lee, "Proc. Int. Conf. on Nuclear Moments and Nuclear Structure", Osaka-Japan, 1972, Ed. H. Horie e K. Sugimoto.

TABLE I

| $r_c$ | Exp. | VB-I | VB-II | MDI-I | ZR | This Work $r_c$ | This Work $r_M$ |
|---|---|---|---|---|---|---|---|
| $Ne^{20}$ | 2.91±0.05[a] | 2.88 | 3.02 | 2.96 | 3.05 | 2.87 | 2.80 |
| $Mg^{24}$ | 2.99±0.03[b] | 3.01 | 3.15 | 3.12 | 3.24 | 3.04 | 2.97 |
| $Si^{28}$ | 3.11±0.03[b] | 3.05 | 3.26 | | 3.35 | 3.16 | 3.09 |
| $S^{32}$ | 3.24±0.03[b] | 3.17 | 3.32 | 3.26 | 3.42 | 3.26 | 3.19 |
| $Ar^{36}$ | | 3.30 | 3.42 | 3.40 | 3.46 | 3.35 | 3.28 |

(a) Ref. 8, (b) Ref. 9.

TABLE II

| $Q_o^C$ | Exp. | VB-I | VB-II | MDI-I | Z R | this work |
|---|---|---|---|---|---|---|
| $Ne^{20}$ | $58 \pm 3$ (a) | 34. | 46. | 45. | 49.8 | 47.9 |
| $Mg^{24}$ | $69 \pm 3$ (a) | 50. | 60. | 50. | 68.6 | 58.9 |
| $Si^{28}$ | $-64 \pm 3$ (a) | -26 | -60 | | -72.2 | -67.8 |
| $S^{32}$ | $47 \pm 3$ (b) | 28. | 52. | 36. | -63.8 | 46.8 |
| $Ar^{36}$ | $54 \pm 6$ (b) | -36 | -48 | -50 | -52.0 | -48.4 |

(a) Ref.10, (b) Ref. 4.

TABLE III

| $H_0^C$ | Exp.(a) | Theor. |
|---|---|---|
| $Ne^{20}$ | $249 \pm 27$ | 127. |
| $Mg^{24}$ | $48 \pm 16$ | -14. |
| $Si^{28}$ | $205 \pm 33$ | 105. |
| $S^{32}$ | | -72. |
| $Ar^{36}$ | | 90. |

(a) Ref.10.

TABLE IV

| | $Ne^{20}$ | $Mg^{24}$ | $Si^{28}$ | $S^{32}$ |
|---|---|---|---|---|
| Exp. | 340 ± 40[a] | 446 ± 45[b] | 346. ± 33[b] | 330. ± 50[c] |
| Eq.(20) | 313. | 453. | 566. | 311. |
| Eq.(21) | 1 7. | 243. | 331. | 131. |
| Ripka | 247. | 470. | 520. | |
| FBB | 204. | 374. | 376. | 325. |

(a) Ref.10, (b) Ref.15, (c) Ref. 16.

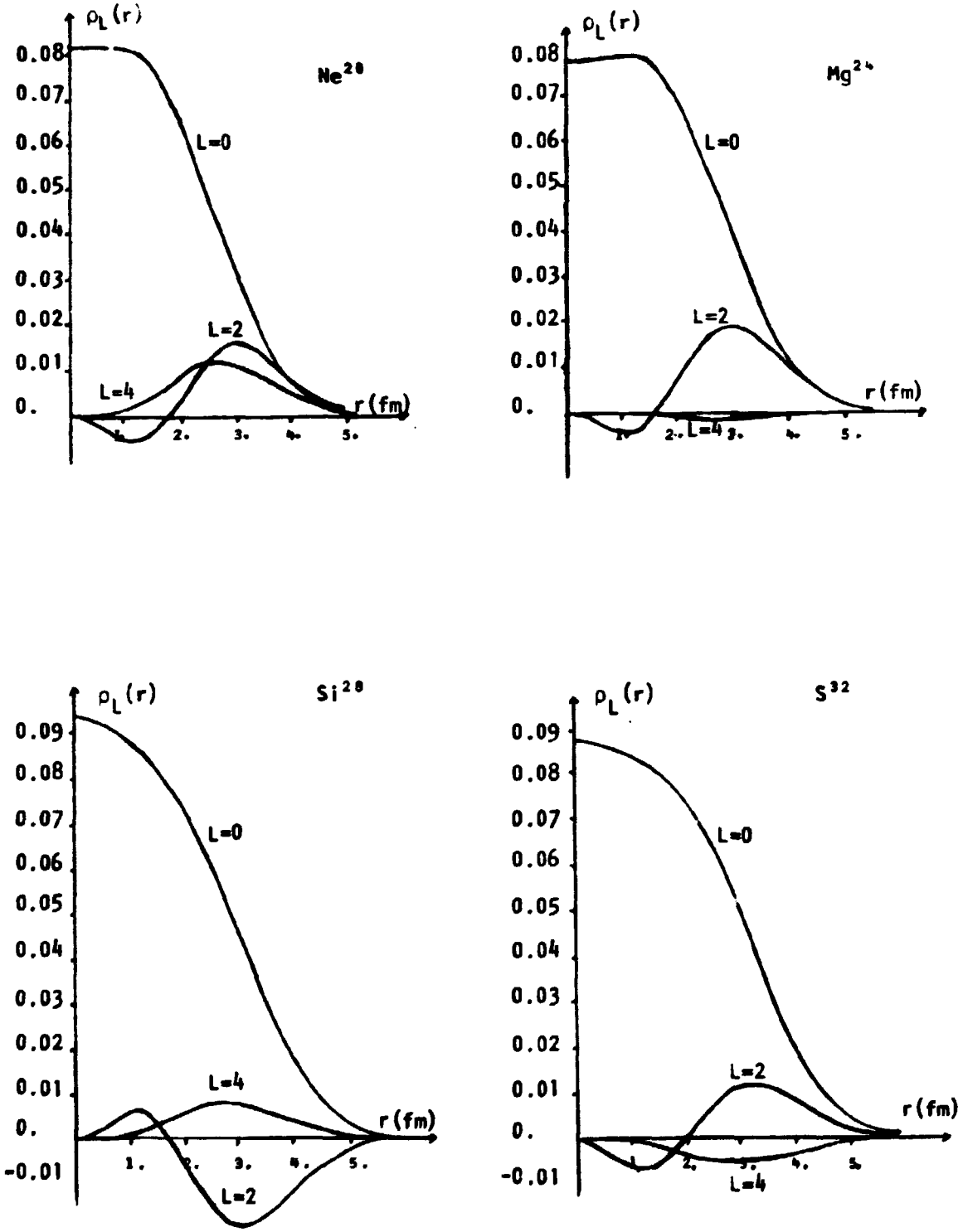
$\rho_L(r)$
$Ne^{20}$
$Mg^{24}$
$Si^{28}$
$S^{32}$
L=0
L=2
L=4
r (fm)
0.08
0.07
0.06
0.05
0.04
0.03
0.02
0.01
0.
0.09
-0.01
1.
2.
3.
4.
5.

FIG.1

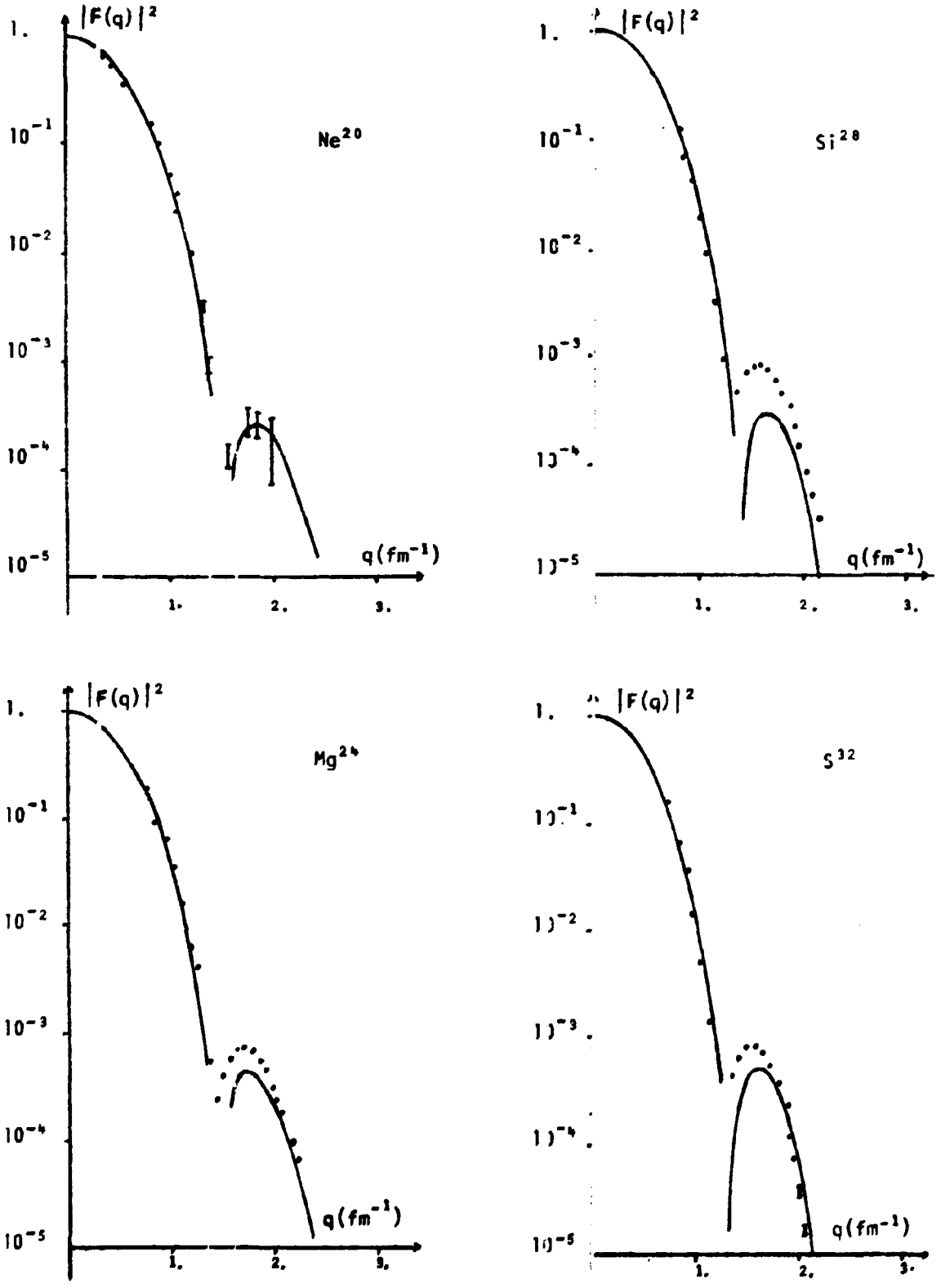


FIG.2

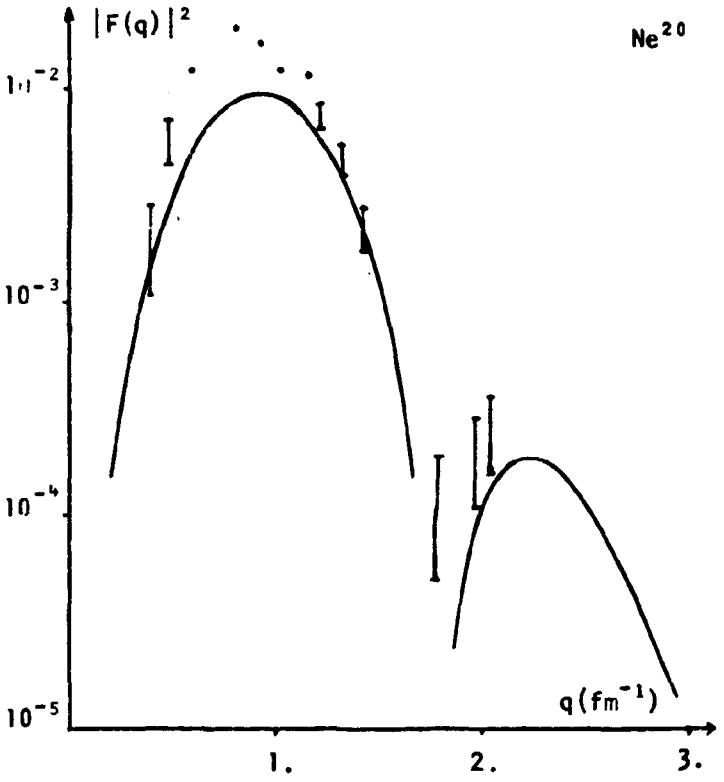
|F(q)|²
Ne²⁰
10⁻²
10⁻³
10⁻⁴
10⁻⁵
q(fm⁻¹)
1.
2.
3.

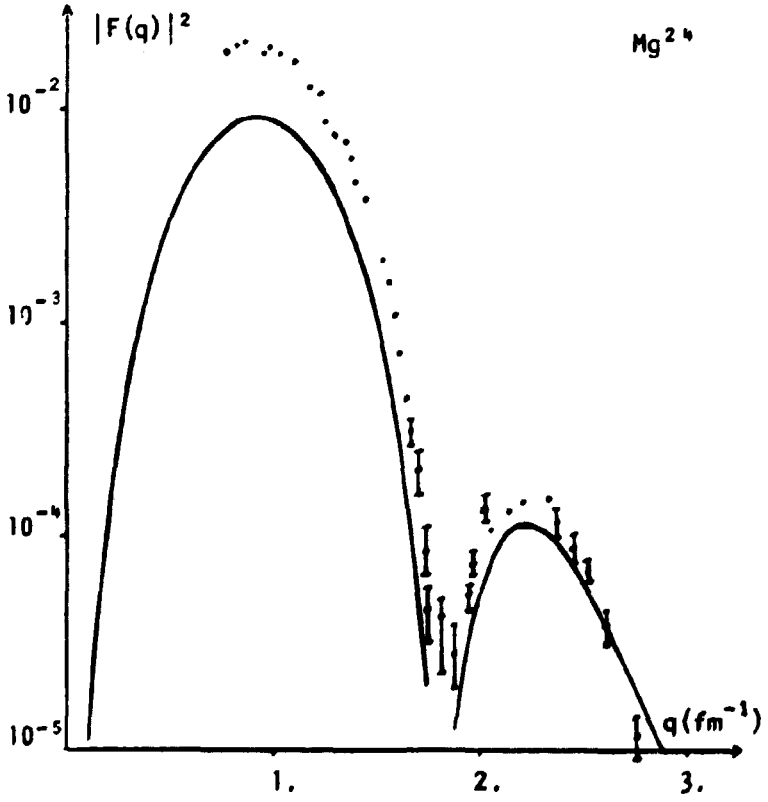
|F(q)|²
Mg²⁴
10⁻²
10⁻³
10⁻⁴
10⁻⁵
q(fm⁻¹)
1.
2.
3.

FIG. 3a

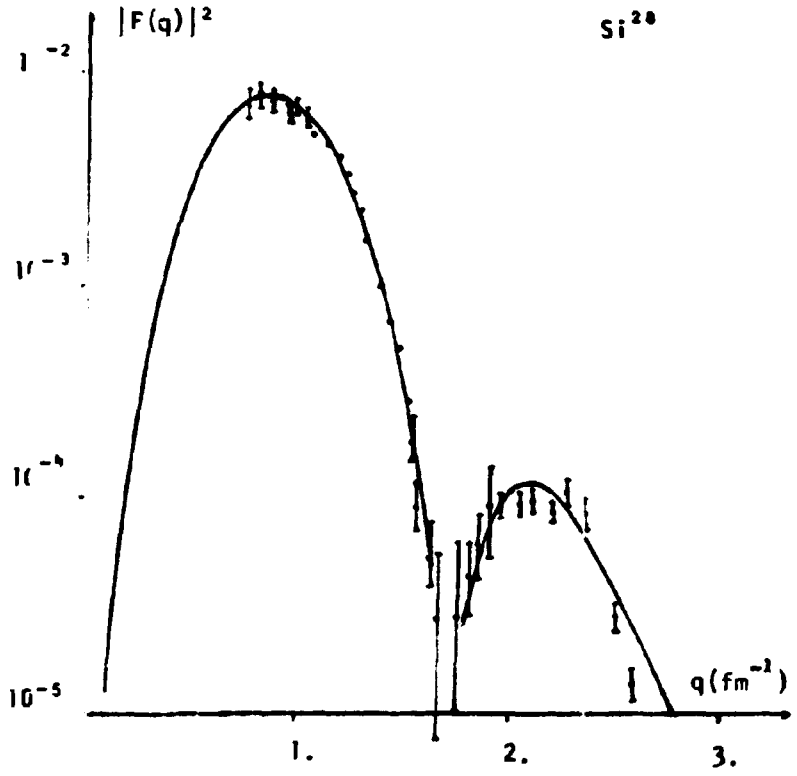


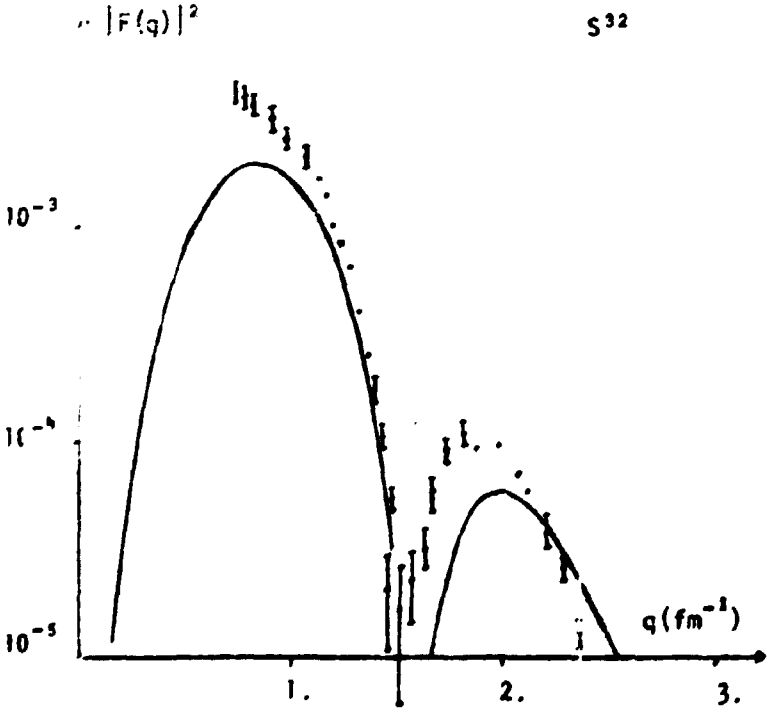


FIG. 3b

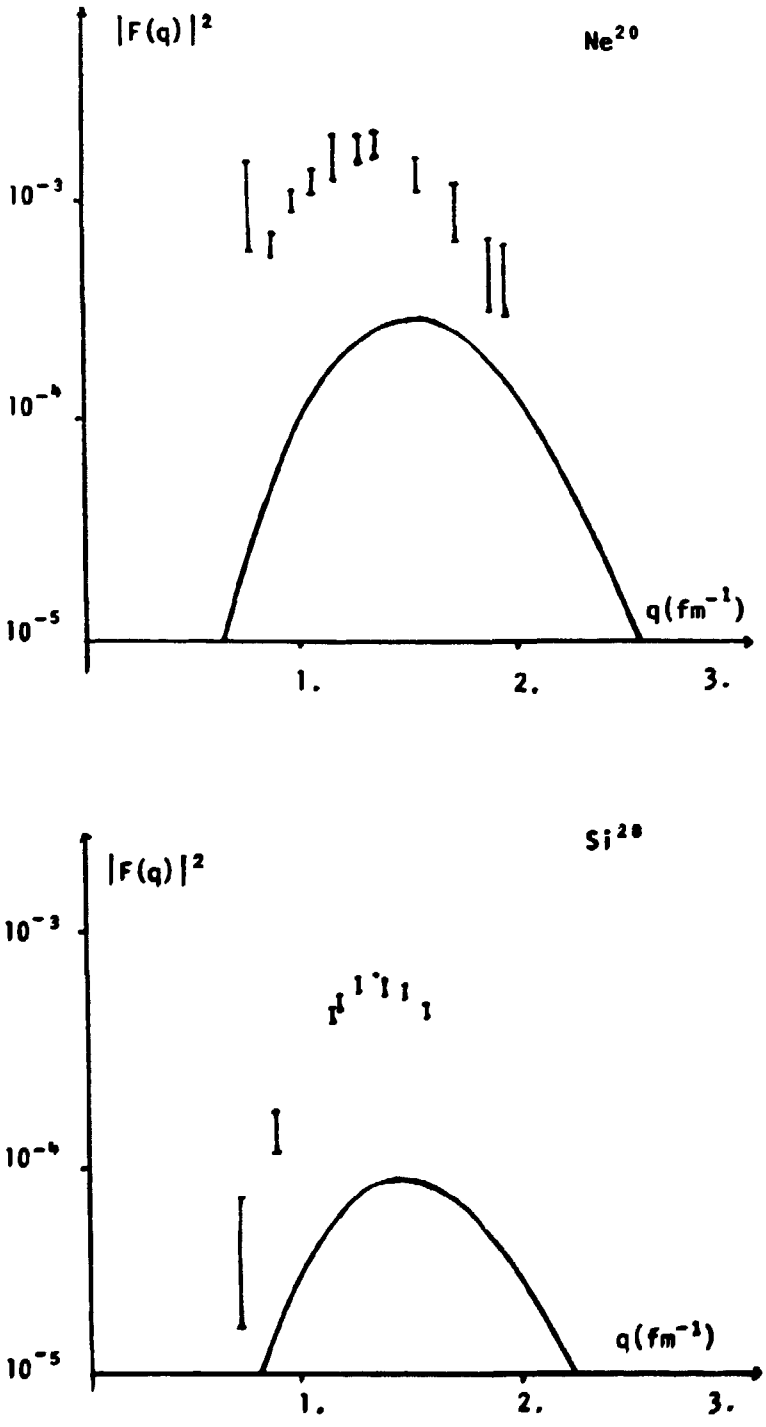


FIG.4

## TABLE CAPTIONS

TABLE I - Nuclear charge radii (in fm) determined by various authors. In the last column we have the mass radius, without the corrections due to the center of mass motion and to the finite size of proton.

TABLE II - Electric quadrupole moments (in $fm^2$) calculated by various authors. In the case of $S^{32}$ and $Ar^{36}$, experiment does not provide their signs.

TABLE III - Electric hexadecapole moments (in $fm^2$) calculated by various authors.

TABLE IV - The $B(E2; 0^+ \longrightarrow 2^+)$ reduced transition probabilities in units of $e^2 fm^4$. Our results from expressions (20) and (21) are in the second and third lines, respectively. The values of Ripka are from Ref.(11). In the last line we have the results of Ford, Braley and Bar-Touv, Ref. (12).

## FIGURE CAPTIONS

Figure 1 - Expansion coefficients of $Ne^{20}$, $Mg^{24}$, $Si^{28}$ and $S^{32}$ nuclear charge density distributions.

Figure 2 - Elastic scattering form factors for $Ne^{20}$, $Mg^{24}$, $Si^{28}$ and $S^{32}$. The points represent experimental values.

Figure 3a - $0^+ \rightarrow 2^+$ inelastic scattering form factors for $Ne^{20}$ and $Mg^{24}$. Experimental values are shown for comparison.

Figure 3b - $0^+ \rightarrow 2^+$ inelastic scattering form factors for $Si^{28}$ and $S^{32}$. Experimental values are also shown.

Figure 4 - $0^+ \rightarrow 4^+$ inelastic scattering form factors for $Ne^{20}$ and $Si^{28}$ with experimental values.